Development 139, 2730-2739 (2012) doi:10.1242/dev.079236

Glycosaminoglycan-dependent restriction of FGF diffusion is necessary for lacrimal gland development

Xiuxia Qu[1], Yi Pan[2], Christian Carbe[1,*], Andrea Powers[1], Kay Grobe[3] and Xin Zhang[1,‡]

SUMMARY

Glycosaminoglycans (GAGs) play a central role in embryonic development by regulating the movement and signaling of morphogens. We have previously demonstrated that GAGs are the co-receptors for Fgf10 signaling in the lacrimal gland epithelium, but their function in the Fgf10-producing periocular mesenchyme is still poorly understood. In this study, we have generated a mesenchymal ablation of UDP-glucose dehydrogenase (Ugdh), an essential biosynthetic enzyme for GAGs. Although *Fgf10* RNA is expressed normally in the periocular mesenchyme, *Ugdh* mutation leads to excessive dispersion of Fgf10 protein, which fails to elicit an FGF signaling response or budding morphogenesis in the presumptive lacrimal gland epithelium. This is supported by genetic rescue experiments in which the *Ugdh* lacrimal gland defect is ameliorated by constitutive Ras activation in the epithelium but not in the mesenchyme. We further show that lacrimal gland development requires the mesenchymal expression of the heparan sulfate *N*-sulfation genes *Ndst1* and *Ndst2* but not the 6-*O* and 2-*O*-sulfation genes *Hs6st1*, *Hs6st2* and *Hs2st*. Taken together, these results demonstrate that mesenchymal GAG controls lacrimal gland induction by restricting the diffusion of Fgf10.

KEY WORDS: FGF, Heparan sulfate, Glycosaminoglycan, Lacrimal gland, Branching morphogenesis, Morphogen gradient, Mouse

INTRODUCTION

Glycosaminoglycans (GAGs) are the major constituents of the extracellular matrix that control the transport and signaling of numerous growth factors (Hacker et al., 2005). Consisting of 50-400 repeats of disaccharide units, GAGs can be divided by their composition, sulfation and epimerization into chondroitin sulfate (CS), dermatan sulfate (DS), heparan sulfate (HS)/heparin, and keratan sulfate (KS). A common precursor of all GAGs is UDP-glucuronic acid, which is synthesized from UDP-glucose by a single mammalian enzyme, UDP-glucose dehydrogenase (Ugdh). Together with an amino sugar such as *N*-acetylglucosamine for HS and *N*-acetylgalactosamine for CS, these monosaccharides are incorporated by polymerization enzymes into the backbone of the polysaccharide and are further modified by a series of sulfotransferase enzymes (Esko and Selleck, 2002). For example, the polymerization of HS is exclusively catalyzed by Ext enzymes, which are followed by *N*-deacetylase/*N*-sulfotransferase (Ndst) enzymes to replace the acetyl group of the glucosamine with a sulfate group. Some of the glucuronic acid (GlcA) residues are next converted by glucuronyl C5-epimerase (Hsepi) into iduronate (IdoA), which can be further sulfated at the C-2 carbon position by the 2-*O*-sulfotransferases (Hs2st). Finally, 3-*O*-sulfotransferases (Hs3st) and 6-*O*-sulfotransferases (Hs6st) complete the secondary modification of HS by sulfating the C-3 and C-6 carbon of the amino sugar residues. As only a subset of the disaccharide residues are processed by these sulfation enzymes, there are enormous heterogeneities among GAG chains that decorate the cell surface. Remarkably, the composition and sulfation pattern of GAGs are highly consistent within each cell type, suggesting that the biosynthesis of GAGs is tightly regulated in a tissue-specific fashion (Maccarana et al., 1996; van Kuppevelt et al., 1998; Ledin et al., 2004).

Fibroblast growth factor (FGF) signaling is among the most studied intercellular pathways that are regulated by GAGs. In particular, HS is known to serve as a co-receptor on the surface of FGF-responding cells, forming a trimeric complex with FGF/FGFR to activate downstream signaling. It remains controversial, however, whether this co-receptor function of HS is dictated by its specific sequence motif or its overall charge content (Kreuger et al., 2006). Nevertheless, biochemical studies have shown that many FGF proteins exhibit preferential binding to specifically sulfated HS, and the selective removal of *N*-, 6-*O*- or 2-*O*-sulfate groups of HS disrupts its interactions with some, but not all FGF-FGFR pairs (Allen and Rapraeger, 2003; Ashikari-Hada et al., 2004). In support of this, we have recently provided genetic evidence that FGF signaling in both lens and lacrimal gland development requires HS biosynthetic enzymes Ndst, Hs6st and Hs2st in vivo (Qu et al., 2011b; Qu et al., 2011a). These results show that the sulfation modification of HS is crucial for its function as a requisite partner of FGFR on the cell surface to detect FGF signals.

Previous studies have also suggested that GAGs might regulate the diffusion of FGFs in the extracellular matrix. It has been observed that FGF family proteins often can bind to highly sulfated GAG sequences, including HS, CS and DS (Jemth et al., 2002; Bao et al., 2004; Kreuger et al., 2005; Taylor et al., 2005). On the one hand, through rapid and reversible binding, cell surface GAGs might protect FGF from proteolytic degradation and control the movement of FGF within the extracellular matrix, thus maintaining the position-dependent gradient of FGF (Beer et al., 1997; Dowd et al., 1999). On the other hand, enzymatic cleavage of GAGs or their attached core protein has been suggested to turn FGF into a long-range signaling molecule by releasing the FGF-bound GAGs. Indeed, it was shown in *Xenopus* embryos that secreted serine protease xHtrA1 stimulated FGF signaling by cleaving GAGs

[1]Department of Medical and Molecular Genetics, Indiana University School of Medicine, Indianapolis, IN 46202, USA. [2]Institute of Nutritional Science, Chinese Academy of Sciences, Shanghai, China. [3]Physiological Chemistry and Pathobiochemistry, University of Muenster, 48149 Münster, Germany.

*Present address: Thomas Jefferson University, Philadelphia, PA, USA
‡Author for correspondence (xz4@iupui.edu)

Accepted 14 May 2012

containing proteoglycans, thus promoting the movement of FGF. Consistent with this, injection of HS and DS in *Xenopus* embryos induced a similar posteriorization effect as that by xHtrA1 and FGF signals (Hou et al., 2007).

The role of GAGs in FGF diffusion during branching morphogenesis is poorly understood. In the vertebrate lung, mesenchymal cells appear to express low-*O*-sulfated heparan HS around the distal tubules, which are undergoing branching morphogenesis, and in whole-lung culture addition of over-*O*-sulfated heparin actually suppressed branching morphogenesis (Izvolsky et al., 2003). However, HS digestion by heparanase in submandibular gland culture was shown to be critical for the release of Fgf10 from the basement membrane and subsequent MAPK signaling (Patel et al., 2007). By contrast, genetic analysis in *Drosophila* demonstrated that, although tracheoblast cells required HS to respond to FGF signaling, ablation of HS in the FGF-producing or surrounding cells did not affect trachea development (Yan and Lin, 2007). These results thus raised questions about the role of HS in the FGF-producing mesenchyme.

The lacrimal gland also develops through branching morphogenesis regulated by FGF signaling. At mouse embryonic day (E) 12.5, the conjunctival epithelium at the temporal side of the mouse eyes invades the Fgf10-expressing mesenchyme to form the initial lacrimal gland bud. The bud elongates posteriorly until E15.5 when secondary branching begins to establish the complex tubuloalveolar structure. This eventually gives rise to the mature lacrimal gland composed of numerous ducts, acini and connective tissue. It has been shown that even heterozygous mutations in *Fgf10* can lead to lacrimal gland aplasia in humans and mice, suggesting that the level of Fgf10 in mesenchyme needs to be precisely modulated in lacrimal gland development (Makarenkova et al., 2000; Entesarian et al., 2005). In this study, we have generated a conditional knockout of *Ugdh* in the periocular mesenchyme to investigate the role of GAG in FGF diffusion. Although the differentiation of the periocular mesenchyme and the expression of the Fgf10 ligand were unaffected, *Ugdh* deletion led to an unrestricted diffusion of Fgf10 in the extracellular matrix. As a result, the presumptive lacrimal gland epithelium failed to activate FGF downstream signaling for a budding response. This is further supported by genetic rescue experiments in which *Ugdh* lacrimal gland defects could be ameliorated by the epithelial but not mesenchymal activation of Ras signaling. Finally, we showed that lacrimal gland development was abrogated by a combined deletion of *Ndst1* and *Ndst2*, but not by a loss of *Hs6st1*, *Hs6st2* and *Hs2st* genes. Therefore, sulfated HS is the crucial component of GAGs in controlling Fgf10 diffusion in lacrimal gland development.

MATERIALS AND METHODS

Mice

The $Ugdh^{flox}$ targeting vector was constructed using the recombineering method from a 12.7 kb genomic fragment (Liu et al., 2003; Carbe et al., 2012), which was retrieved from a C57BL/6 bacterial artificial chromosome (BAC) clone (RP23-477N9, BACPAC Resources Center at Children's Hospital Oakland Research Institute, CA, USA). It contains a neomycin (*Neo*) selection cassette surrounded by two *frt* sites and exon 6 of the *Ugdh* gene flanked by two *loxP* sites (Fig. 1A). The linearized targeting construct was electroporated into 129S6/SvEvTac embryonic stem (ES) cells and recombinant clones were screened by Southern blot analysis with 5′ (*Sac*I) and 3′ (*Bam*HI) external probes before being injected into C57BL/6 blastocysts. Chimeras were further bred with C57BL/6 mice for germline transmission, which was confirmed by PCR genotyping using the following primers: $Ugdh^{flox}F$: 5′-TTCTGAGGCTGTATTTCACTTCC-3′; $Ugdh^{flox}R$: 5′-AGGCACAGGCACGATTAGGA-3′. The amplification bands of 214 bp and 314 bp corresponded to the wild-type and flox alleles, respectively. After crossing with an *Flpe* transgenic line (stock number 009086, Jackson Laboratory, Bar Harbor, ME, USA), the *frt*-flanked *Neo* cassette was removed in the $Ugdh^{flox}$ mice.

$Ndst1^{flox}$ and $Hs6st2^{KO}$ mice were described previously (Grobe et al., 2005; Qu et al., 2011b). $Hs6st1^{flox}$ is a kind gift from Dr Wellington V. Cardoso (Boston University School of Medicine, Boston, MA, USA) (Izvolsky et al., 2008). $Hs2st^{flox}$ is a kind gift from Dr Jeffrey D. Esko (University of California San Diego, La Jolla, CA, USA) (Stanford et al., 2010). $Tg\text{-}Hras^{G12V}$ is a kind gift from Dr Paul A. Overbeek (Baylor College of Medicine, Houston, TX, USA) (Burgess et al., 2010). $Ndst2^{KO}$ is a kind gift from Dr Lena Kjellén (University of Uppsala, Uppsala, Sweden) (Forsberg et al., 1999). The P6 5.0 *lacZ* reporter transgenic mice were kindly provided by Drs Paul A. Overbeek and Richard Lang (Children's Hospital Research Foundation, Cincinnati, OH, USA) (Makarenkova et al., 2000). $LSL\text{-}Kras^{G12D}$ mice were obtained from the Mouse Models of Human Cancers Consortium (MMHCC) Repository at National Cancer Institute (Tuveson et al., 2004). *Wnt1-Cre* mice were from Jackson Laboratory (stock number 009107) (Danielian et al., 1998). The *Wnt1*-Cre*;* $Ugdh^{flox/flox}$ embryos were generated by crossing *Wnt1*-Cre*;* $Ugdh^{flox/+}$ animals with $Ugdh^{flox/flox}$ mice, and the *Wnt1*-Cre*;* $Ugdh^{flox/+}$ embryos in the same litter were used as wild-type controls. The animals were maintained in mixed genetic backgrounds. All experiments were performed in accordance with institutional guidelines.

Histology and immunohistochemistry

Hematoxylin and Eosin (H&E) histology, carmine staining and immunohistochemistry were performed as previously described (Pan et al., 2008). For HS detections, sections were treated with 50 U/μl heparintinase I (Seikagaku, Tokyo, Japan) for 2 hours at 37°C to expose the terminal desaturated hexuronate residues at the non-reducing ends of HS, which are recognizable by 3G10 antibody (David et al., 1992). By contrast, 10E4 antibody binds HS epitopes that are *N*-sulfated and *N*-acetylated rather than *O*-sulfated (David et al., 1992; van den Born et al., 2005). For phospho-ERK staining, the Tyramide Signal Amplification kit (TSA Plus System, PerkinElmer, Waltham, MA, USA) was used to amplify the signal. The following antibodies were used: anti-phospho-ERK1/2 (#4370, Cell Signaling Technology, Beverly, MA, USA), 10E4 (Seikagaku, Tokyo, Japan). 3G10 (#H1890-75, United States Biological, Swampacott, MA, USA), anti-chondroitin sulfate (#C8035, Sigma, St Louis, MO, USA), anti-E-cadherin (U3254, Sigma), anti-Fgf10 (#sc-7917, Santa Cruz Biotechnology, Santa Cruz, CA, USA), anti-Pax6 (PRB-278P, Covance, Berkeley, CA, USA). At least three embryos of each genotype were analyzed.

RNA in situ hybridization

RNA in situ hybridization on cryosections was performed according to a standard protocol (Pan et al., 2008). Briefly, the digoxigenin-labeled probe was hybridized on cryosections overnight at 65°C, followed by stringent washing. After equilibration with maleic acid buffer, the sections were incubated with an AP-conjugated anti-digoxigenin antibody (Roche, Indianapolis, IN, USA) at 4°C overnight. Hybridization signals were visualized with BM Purple (Roche) and photographed under a Leica DM3000 microscope. The following probes were used: *Erm* (*Etv5* – Mouse Genome Informatics) and *Er81* (*Etv1* – Mouse Genome Informatics) (both from Dr Bridget Hogan, Duke University Medical Center, Durham, NC, USA), *Pitx2* (from Dr Valerie Dupé, CNRS, Strasbourg, France), *Crabp1* and *FoxC1* (from Dr Anthony Firulli, Indiana University School of Medicine, Indianapolis, IN, USA). *Fgf10* and *Dusp6* probes were generated from full-length cDNA clones (IMAGE: 6313081 and 3491528, Open Biosystems, Huntsville, AL, USA). At least three embryos of each genotype were analyzed for each probe.

FGF ligand and carbohydrate engagement assay (LACE)

The LACE assay was performed as previously described (Pan et al., 2008). Briefly, cryosections or deparaffinized paraffin sections were treated with 0.5 mg/ml $NaBH_4$ for 10 minutes and 0.1 M glycine for 30 minutes, followed by 1 hour blocking with 2% bovine serum albumin (BSA) at room temperature. After blocking, the sections were incubated with a mixture of 20 μM Fgf10 and 20 μM human FGFR-Fc chimera (R&D Systems, Minneapolis, MN, USA) in RPMI-1640 with 10% fetal bovine serum (FBS) at 4°C overnight. Signal was detected by immunofluorescence with Cy3-labeled anti-human Fc IgG antibody. The assay was repeated on at least three embryos of each genotype.

Western blot

The periocular tissue was dissected from E13.5 embryos and homogenized in RIPA buffer with protease inhibitors. After quantification by BCA protein assay kit (Pierce, Rockford, IL, USA), equal amounts of protein were loaded and separated on 15% SDS-PAGE gels before being transferred to Millipore Immobilon FL PVDF membranes (Millipore, Billerica, MA, USA). The membranes were blocked for 1 hour in Odyssey blocking reagent and incubated overnight with 1:200 diluted anti-Fgf10 antibody (#sc-7917, Santa Cruz Biotechnology) and 1:2000 diluted anti-ERK1/2 antibody (#4695, Cell Signaling Technology) at 4°C. After further incubation with IRDye linked anti-rabbit secondary antibody, the membrane was scanned and quantified using the Odyssey SA system (LICOR Biosciences, Lincoln, NE, USA).

Fgf10 diffusion assay

Heads of E10.5 embryos were cut and divided sagittally at the midline. One hundred to two hundred mesh Affi-Gel blue Gel beads (#153-7302, Bio-Rad, Hercules, CA, USA) soaked with 5 mg/ml BSA or 500 μg/ml recombinant Fgf-10 (R&D Systems) were inserted into the mesenchyme around the eye region. Limb buds were also dissected from E10.5 embryos and implanted with beads. Tissue was laid flat on Millipore filters (Nitrocellulose Membrane Black Gridded, filter type 0.45 μm) floating on DMEM (Gibco, Carlsbad, CA, USA) culture medium and incubated for 3 hours in a tissue culture incubator at 37°C with 5% CO_2 as described (Harada et al., 2009). Explants were fixed in 4% paraformaldehyde (PFA) for 3 hours, embedded in optimal cutting temperature compound (OCT) and processed for Fgf10 staining. The maximum diffusion range of each sample was measured using the imageJ program and statistical significance was calculated using the one-way ANOVA analysis with Tukey's multiple comparison test.

Lacrimal gland induction assay

Embryos carrying the P6 5.0 *lacZ* reporter line at E13.5-14.5 stages were used to perform the lacrimal gland induction assay as described previously (Pan et al., 2008). Briefly, Fgf10 (R&D Systems) or BSA-soaked heparin acrylic beads (Sigma) were placed in the periocular mesenchyme. Explants were cultured for 48 hours in a tissue culture incubator, floating on a filter paper (Nitrocellulose Membrane Black Gridded, 0.45 μm pore, Millipore) in the culture medium [CMRL-1066 supplemented with 10% FBS, 4 mM L-Glutamine, 0.1 mM non-essential amino acids and antibiotics (Gibco)]. The *lacZ*-expressing lacrimal gland buds were stained with X-gal and photographed under a Leica MZ16F dissecting microscope. Fisher's exact test was used to calculate statistical significance.

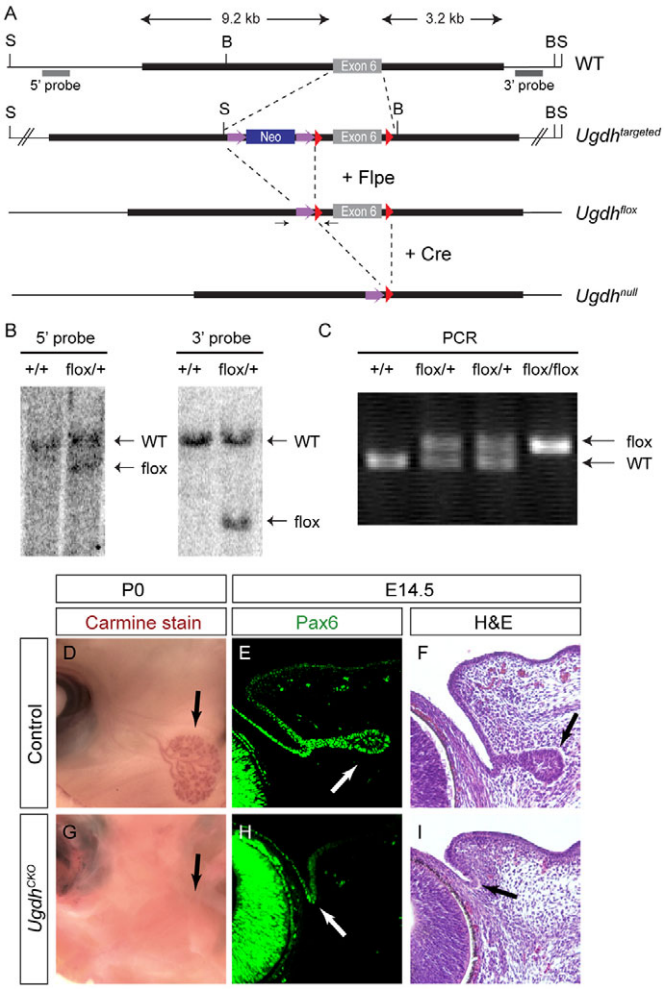

Fig. 1. Mesenchymal ablation of *Ugdh* disrupted lacrimal gland development. (**A**) Schematic of $Ugdh^{flox}$ allele. Through homologous recombination, an *frt*-flanked *Neo* cassette and two *loxP* sites were inserted next to the exon 6 of the *Ugdh* gene. After the *Neo* selection cassette was removed by mating with the *Flpe* mice, the $Ugdh^{flox}$ allele was left with two *loxP* sites flanking the *Ugdh* exon 6, which can be deleted via Cre-mediated recombination. S, *Sac*I; B, *Bam*HI; purple arrows, *frt* site; red triangle, *loxP* site. (**B**,**C**) The gene targeting was confirmed by Southern blots using 5′ (*Sac*I) and 3′ (*Bam*HI) probes, and by genotype PCR using the $Ugdh^{flox}F$ and $Ugdh^{flox}R$ primers. (**D-I**) *Wnt1-Cre* mediated ablation of *Ugdh* (*Wnt1*-Cre; $Ugdh^{flox/flox}$ or $Ugdh^{CKO}$) resulted in a loss of lacrimal glands at birth, as shown by carmine staining (D,G, arrows). At E14.5, no budding of lacrimal glands was observed in the *Ugdh* mutants as shown by Pax6 staining (E,H, arrows) and H&E histology (F,I, arrows).

RESULTS

Mesenchymal Ugdh is required for lacrimal gland development

Ugdh is a biosynthetic enzyme for UDP-glucose, a substrate required for all GAG synthesis. To investigate the general function of GAG in embryonic development, we constructed a conditional allele of *Ugdh* by inserting two *loxP* sites flanking the *Ugdh* exon 6, which encodes its catalytic domain (Fig. 1A) (Campbell et al., 2000; Sommer et al., 2004). Homologous recombination in ES cells was identified by Southern blots using both the 5′ and 3′ probes and germline transmission was confirmed by PCR using primers that surround the 5′ *loxP* site (Fig. 1B,C). $Ugdh^{flox/flox}$ mice were born healthy at the normal Mendelian ratio and were fertile as adults, indicating that the conditional allele had no overt hypomorphic effects.

We have previously shown that *Wnt1-Cre* mediated ablation of *Ndst1*, an HS biosynthetic enzyme, disrupted the sulfation pattern of HS in the periocular mesenchyme (Pan et al., 2008). Interestingly, no lacrimal gland phenotype was observed in this animal model, suggesting that lacrimal gland development did not require mesenchymal modification of HS by Ndst1. To investigate further

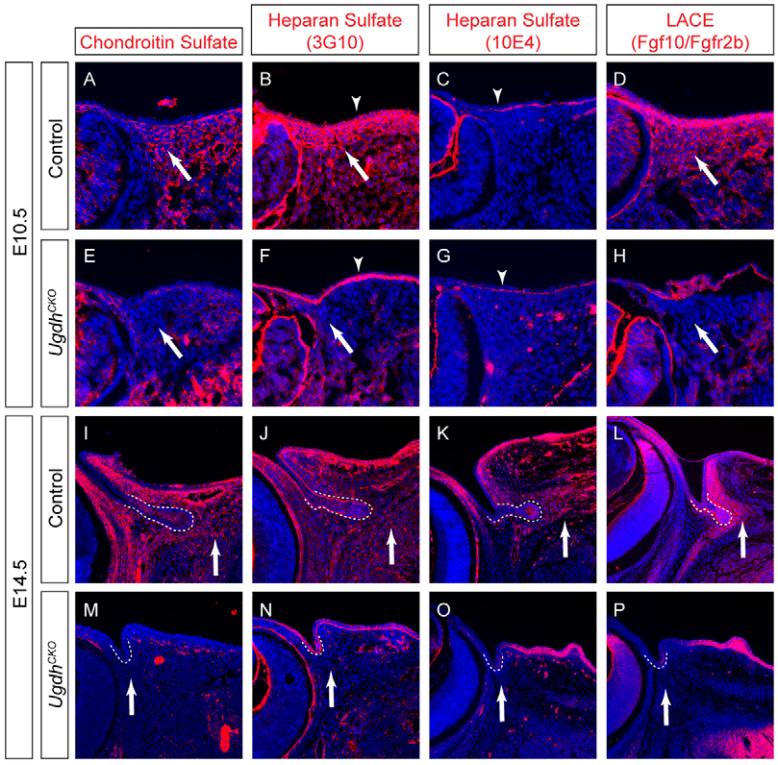

Fig. 2. *Ugdh* deletion abolished GAG synthesis. (**A-H**) At E10.5, the *Ugdh*^{CKO} mutants lost CS and HS (3G10) staining in the mesenchyme (A,B,E,F, arrows). There was little HS 10E4 staining in the mesenchyme at this stage (C,G), but the LACE staining of Fgf10/Fgfr2b, which was specific to sulfated HS, was also lost in the *Ugdh* mutant mesenchyme (C,D,G,H, arrows). Notice that the epithelial HS 3G10 and 10E4 staining was maintained (B,C,F,G, arrowheads). (**I-P**) At E14.5, the *Ugdh* mutant mesenchyme lost all CS and HS (3G10, 10E4 and LACE) staining (arrows). The lacrimal gland primordia were outlined in white.

the role of GAGs in lacrimal gland development, we crossed *Wnt1-Cre* mice with the *Ugdh*^{flox} allele to deplete all GAGs in the periocular mesenchyme. The *Wnt1*-Cre*; Ugdh*$^{flox/flox}$ (hereafter referred to as *Ugdh*^{CKO}) mice were born with a normal body size but died at birth with craniofacial defects including cleft palate (data not shown). In contrast to the *Wnt1*-Cre*; Ndst1*$^{flox/flox}$ mutants, carmine staining further revealed a complete absence of the lacrimal gland in the *Ugdh*^{CKO} pups (Fig. 1D,G, arrows). The lacrimal gland develops at mid-gestation through budding morphogenesis from the conjunctival epithelium, which can be identified by Pax6 expression (Fig. 1E,F, arrows). In the E14.5 *Ugdh*^{CKO} embryos, however, no such buds were ever observed (Fig. 1H,I, arrows; see Fig. 6F for statistics). Therefore, lacrimal gland development requires *Ugdh* function in the periocular mesenchyme.

Ugdh ablation disrupted the biosynthesis of GAGs

To determine the mechanism of *Ugdh* function, we next examined the biosynthesis of GAGs in the *Ugdh*^{CKO} mutants. Using an antibody specific to CS, we observed that at E10.5 this major family of GAGs was expressed in the control periocular mesenchyme but lost in the *Ugdh*^{CKO} mutants (Fig. 2A,E, arrows). Another major GAG, HS, can be detected by the antibody 3G10, which recognizes a common stub motif present in all HS after heparintinase I digestion (Pan et al., 2006). We showed that 3G10 staining was also lost in the *Ugdh* mutant mesenchyme but preserved in the epithelium (Fig. 2B,F, arrows and arrowheads). Consistent with this, both control and mutant embryos at E10.5 expressed *N*-sulfated HS recognized by the 10E4 antibody in the basement membrane of the epithelium but not in the mesenchyme (Fig. 2C,G, arrowheads) (Pan et al., 2006). Finally, we have previously shown that the assembly of the high affinity Fgf10/Fgfr2b complex on the cell surface required HS with selective secondary modifications, which could be detected by the FGF ligand and carbohydrate engagement assay (LACE) (Qu et al., 2011b). In E10.5 *Ugdh*^{CKO} mutants, the Fgf10/Fgfr2b LACE signal was again lost specifically in the periocular mesenchyme (Fig. 1D,H, arrows), consistent with the HS defects seen in early *Ugdh*^{CKO} embryos.

These results were further confirmed at E14.5 when the lacrimal gland bud had already extended from the fornix of the conjunctival epithelium in control embryos. In contrast to strong expression of GAGs in the control mesenchyme that surrounded the lacrimal gland bud, the *Ugdh*^{CKO} mutants lost CS and HS staining in the periocular mesenchyme underneath the conjunctival epithelium (Fig. 2I-P, arrows). Taken together, these results showed that the *Wnt1-Cre* mediated ablation of *Ugdh* indeed disrupted the expression of CS and HS in the periocular mesenchyme, confirming the essential role of Ugdh in GAG synthesis.

Ugdh mutants preserved *Fgf10* expression but lost FGF signaling in lacrimal gland development

The profound loss of GAGs in the *Ugdh*^{CKO} mutants prompted us to ask whether development of the periocular mesenchyme was also affected. At E10.5 when GAGs were already depleted in the mutant periocular mesenchyme, we still detected in the *Ugdh*^{CKO} mutants the specific expression of *Crabp1*, *FoxC1* and *Pitx2*, all markers of ocular anterior segment development (Fig. 3A-F, arrows). At E12.5, *Ugdh*^{CKO} mutants not only preserved a similar expression of *Crabp1*, *FoxC1* and *Pitx2* as the control, but also displayed correct expression of *Fgf10* in the periocular mesenchyme underneath the invaginating conjunctival epithelium (Fig. 3G-J, arrows; data not shown). Moreover, we failed to detect any statistically significant difference in cell proliferation as indicated by BrdU incorporation and Ki67 staining between the control and mutants (data not shown). Therefore, the *Ugdh*^{CKO} mutant mesenchyme appeared be properly developed at the time of lacrimal gland induction.

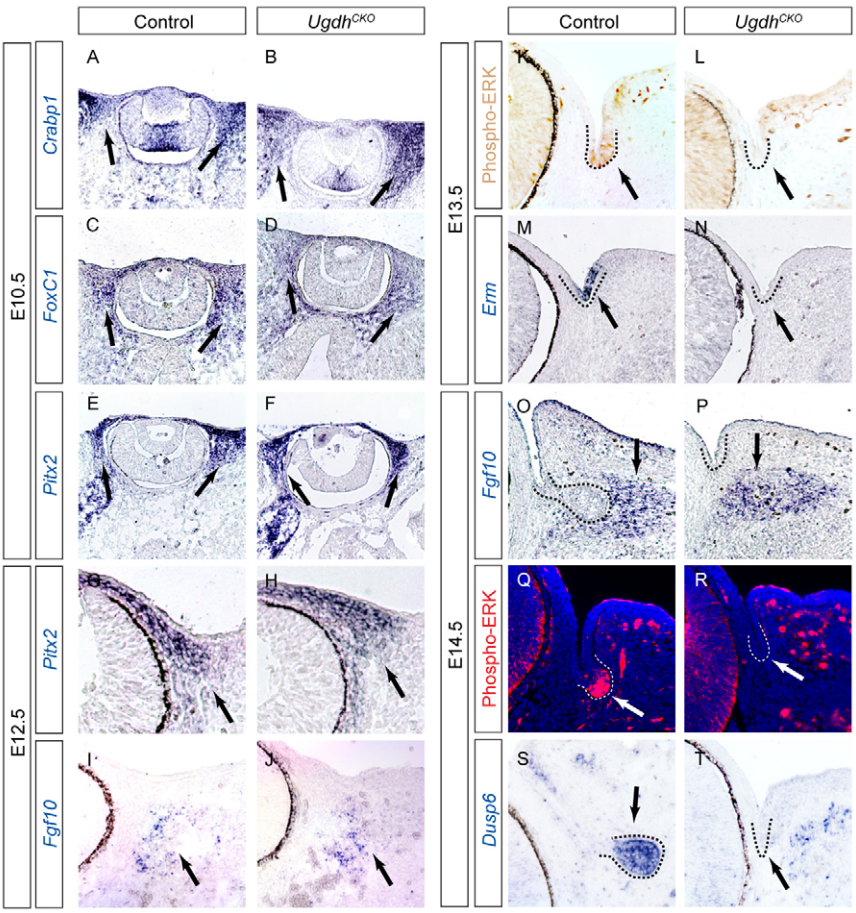

Fig. 3. The *Ugdh* mutants preserved the mesenchymal *Fgf10* expression but lost the epithelial FGF signaling in lacrimal gland development. (**A-J**) RNA in situ hybridization showed that the periocular markers *Crabp1*, *FoxC1* and *Pitx2* were unaffected in E10.5 and E12.5 $Ugdh^{CKO}$ mutants (A-H, arrows). Similarly, *Fgf10* remained expressed in the *Ugdh* mutant mesenchyme adjacent to the epithelium (I,J, arrows). (**K-T**) At E13.5, lacrimal gland progenitors in the control conjunctival epithelium expressed FGF signaling markers, phospho-ERK and *Erm* (K,M, arrows). These expressions were lost in the $Ugdh^{CKO}$ mutants (L,N, arrows). Similarly, despite the unchanged *Fgf10* expression, lacrimal gland buds, which stained positive for phospho-ERK and *Dusp6*, were detected only in the E14.5 control embryos but not in the *Ugdh* mutants (O-T, arrows).

Despite the apparently normal expression of *Fgf10* in the *Ugdh* mutant mesenchyme, we observed a complete loss of FGF signaling during lacrimal gland development. In E13.5 control embryos, lacrimal gland progenitors first appeared as a patch of thickening cells at the fornix of the conjunctival epithelium, which exhibited elevated phosphorylation of ERK, a downstream mediator of FGF signaling, and increased expression of *Erm*, an FGF signaling downstream response gene (Fig. 3K,M, arrows). In the $Ugdh^{CKO}$ mutants, however, both ERK phosphorylation and *Erm* expression were abolished in the presumptive lacrimal gland progenitor cells (Fig. 3L,N, arrows). Similarly, strong activation of FGF signaling was evident in the E14.5 control lacrimal gland bud by robust expression of phospho-ERK and *Dusp6*, another FGF signaling inducible gene. By contrast, the $Ugdh^{CKO}$ mutants preserved *Fgf10* expression in mesenchyme but failed to display any phospho-ERK and *Dusp6* staining in the conjunctival epithelium (Fig. 3O-T, arrows). These results suggest that the *Ugdh* lacrimal gland defects might be caused by the loss of FGF signaling.

Excessive Fgf10 diffusion disrupted lacrimal gland budding in *Ugdh* mutants

GAGs in the extracellular matrix might promote cell signaling by protecting growth factors from degradation or by restricting their dispersion. To test these ideas, we first collected periocular mesenchyme from E13.5 embryos and performed western blots. As shown in Fig. 4A,B, both control and $Ugdh^{CKO}$ mutants exhibited comparable amounts of Fgf10 protein expression in the periocular mesenchyme, suggesting that GAGs were not required for the stability of Fgf10 protein in lacrimal gland development. We next performed an FGF diffusion assay to determine whether the extracellular GAG regulated Fgf10 dispersion. As the endogenous expression of Fgf10 protein was below the detection limit of immunohistochemistry (data not shown), we decided to implant E10.5 head explants with beads soaked with either BSA or Fgf10 in the periocular mesenchyme. After culturing for 3 hours, a ring of Fgf10 immunostaining could be detected in the control explants closely encircling the Fgf10 beads but not the BSA beads (Fig. 4C,F). By contrast, the $Ugdh^{CKO}$ mutants exhibited a much wider span of Fgf10 immunostaining surrounding the Fgf10 beads in the periocular mesenchyme (Fig. 4D,G). However, both the control and $Ugdh^{CKO}$ mutants displayed limited Fgf10 diffusion in the limb mesenchyme (Fig. 4E,H,I), which does not contain *Wnt1-Cre* derived neural crest (data not shown). These results suggested that *Ugdh* mutation led to an expanded diffusion of Fgf10 in the periocular mesenchyme.

We reasoned that excessive dispersion of Fgf10 in *Ugdh* mutant mesenchyme would probably lower its local concentration, effectively reducing the inductive strength of Fgf10 in promoting lacrimal gland budding. We thus performed a lacrimal gland induction assay to assess the potency of Fgf10 signaling in ex vivo explant culture. To visualize the budding of the lacrimal gland, we crossed our animals with P6 5.0 *lacZ* transgenic mice, which express the *lacZ* reporter under the control of a *Pax6* promoter in the lacrimal gland (Makarenkova et al., 2000). In control explants of E13.5-E14.5 embryos, endogenous lacrimal glands stained by X-gal could be observed to grow spontaneously from the eye rudiments, unperturbed by BSA-soaked beads in the periocular

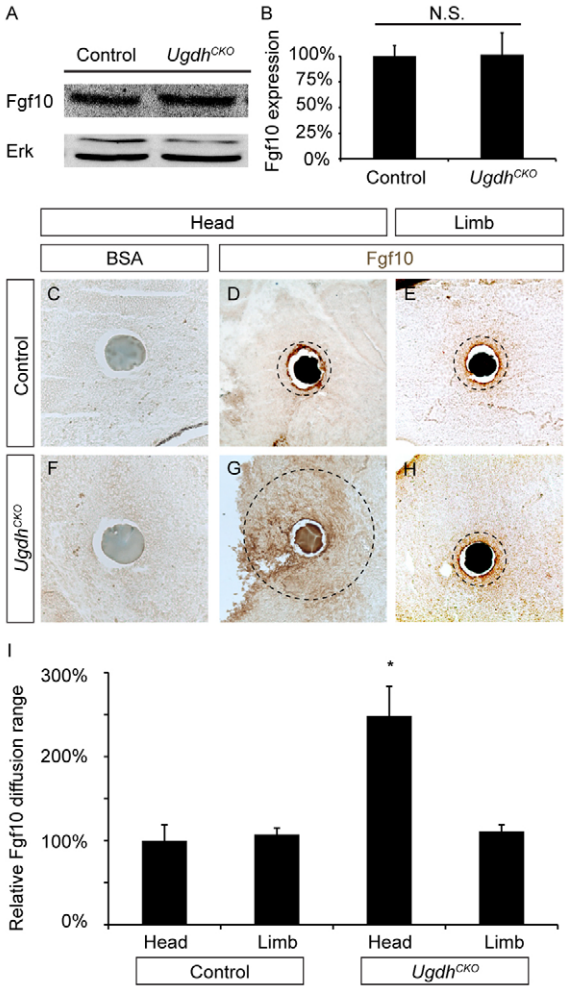

Fig. 4. Expanded Fgf10 diffusion in the *Ugdh* mutants. (**A**,**B**) Western blots of E13.5 periocular mesenchyme showed that the Fgf10 protein was expressed at similar levels in control and $Ugdh^{CKO}$ mutants. After normalization using ERK proteins in the same lysates, Fgf10 expression in the $Ugdh^{CKO}$ mutants (n=5) was plotted as the percentage of the average Fgf10 expression in controls (n=8). (**C-H**) In E10.5 control explant cultures, immunohistochemistry showed limited diffusion of Fgf10 proteins around Fgf10-soaked beads but not BSA-soaked beads in the periocular mesenchyme. The diffusion of Fgf10 proteins was significantly expanded in the *Ugdh* mutant explants. In the limb mesenchyme, the ranges of Fgf10 diffusion were similar in both the control and *Ugdh* mutants. Fgf10 immunostaining was circled in black. (**I**) The Fgf10 diffusion range was quantified by measuring the longest distance reached by Fgf10 staining from the center of the beads in control (n=18 for head, n=37 for limb) and *Ugdh* mutant (n=22 for head, n=22 for limb) explants. *P<0.001.

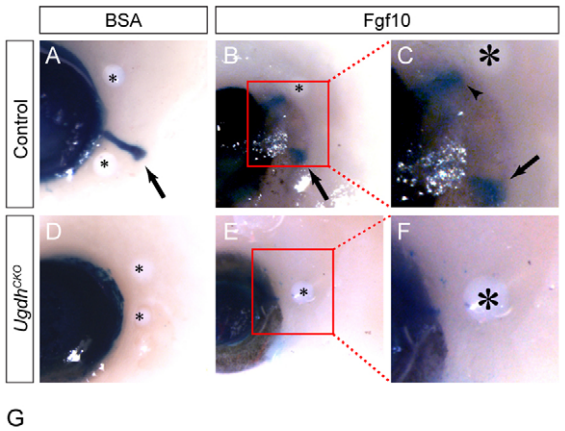

G

		The efficiency of lacrimal gland budding (%)		
		Endogenous	Ectopic	(# of explants)
Control	BSA	100%	0%	(12)
	Fgf10	84%	51%	(51)
$Ugdh^{CKO}$	BSA	0%	0%	(6)
	Fgf10	6%	6%*	(18)

*P<0.001

Fig. 5. Fgf10-induced lacrimal gland budding was abolished in the *Ugdh* mutants. (**A-F**) In E13.5 control explant culture, BSA-containing beads did not perturb budding of the endogenous lacrimal gland (A, arrow), whereas Fgf10-containing beads induced ectopic lacrimal gland buds (B, enlarged in C, arrowhead). By contrast, this ectopic induction of lacrimal gland buds was disrupted in $Ugdh^{CKO}$ mutant explants (D-F). Beads are marked by asterisks. Endogenous and ectopic buds are marked by arrows and arrowhead, respectively. (**G**) The efficiency of lacrimal gland budding in explant cultures.

mesenchyme (Fig. 5A, arrow). By contrast, lacrimal gland budding was disrupted in the $Ugdh^{CKO}$ mutant explants (Fig. 5D). As we and others have shown previously, Fgf10-soaked beads were able to efficiently induce ectopic lacrimal gland buds from the control eye rudiments (Fig. 5B,C, arrows) (Makarenkova et al., 2000; Pan et al., 2008). In the $Ugdh^{CKO}$ mutant explants, however, the efficiency of ectopic lacrimal gland budding was significantly reduced (Fig. 5E-G, P<0.001). Therefore, the loss of GAGs in periocular mesenchyme disrupted Fgf10-induced lacrimal gland budding in the $Ugdh^{CKO}$ mutants.

Epithelial Ras signaling rescued the lacrimal gland budding defects in the mesenchymal *Ugdh* mutants

The above results suggest that GAGs restrict the diffusion of Fgf10 in the periocular mesenchyme, which is necessary for budding of the lacrimal gland from conjunctival epithelium. This non-cell-autonomous model predicts that lacrimal gland defects caused by GAG deficiency in the mesenchyme could be rescued by the restoration of FGF downstream signaling in the epithelium. To test this model, we crossed the $Ugdh^{CKO}$ mutant with two transgenic lines that expressed the constitutively active forms of Ras, which is a major downstream mediator of FGF signaling. Driven by the same *Pax6* promoter used in the P6 5.0 *lacZ* transgenic mice, the $Tg\text{-}Hras^{G12V}$ line expressed the activated *Hras* (G12V) specifically in the lens and conjunctival epithelium (Fig. 6A) (Burgess et al., 2010). In the $LSL\text{-}Kras^{G12D}$ mouse, however, oncogenic *Kras* expression was controlled by its endogenous promoter but blocked by a floxed transcription stop cassette (Fig. 6A) (Tuveson et al., 2004). When crossed with the $Ugdh^{CKO}$ (*Wnt1-Cre;* $Ugdh^{flox/flox}$) mice, this stop cassette was expected to be cleaved by the *Wnt1-Cre* deleter, which also disrupted the $Ugdh^{flox}$ allele. This would result in a simultaneous ablation of GAG and activation of Kras signaling in the periocular mesenchyme. We have previously demonstrated that this strategy could compensate for the loss of FGF signaling in retinal, lens and lacrimal gland development (Cai et al., 2010; Pan et al., 2010; Qu et al., 2011a). Nevertheless, no

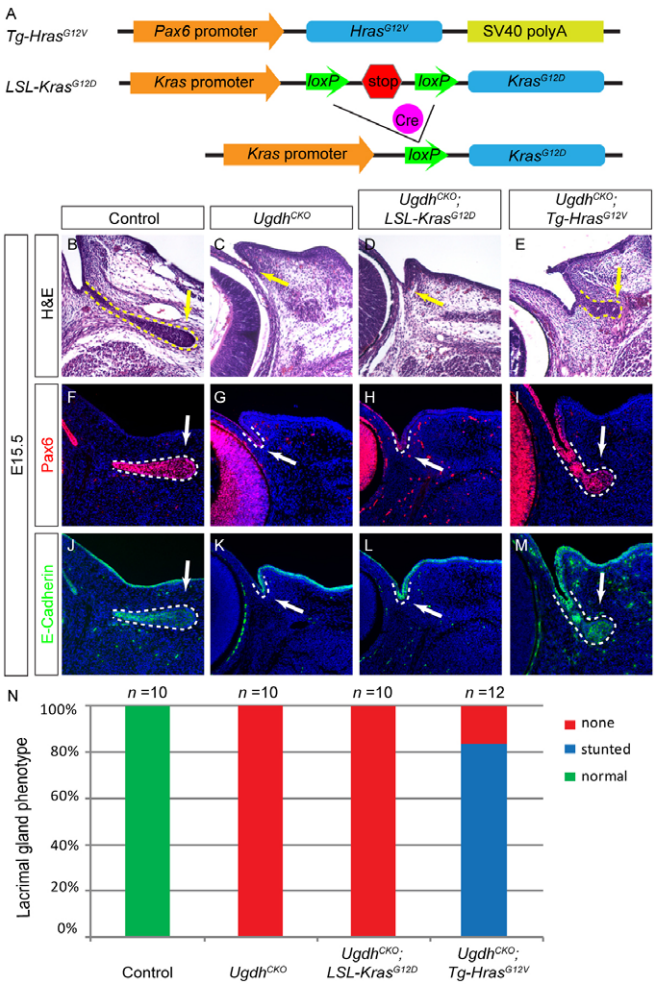

Fig. 6. The lacrimal gland budding defects in the *Ugdh* mutants were rescued by the activated Ras signaling in epithelium but not in mesenchyme. (**A**) Schematic of *Tg-Hras*^{G12V} and *LSL-Kras*^{G12D} mouse lines. *Tg-Hras*^{G12V} was driven by a *Pax6* promoter specifically in the lacrimal gland epithelium, whereas *LSL-Kras*^{G12D} was inducible in mesenchyme only when crossed with *Wnt1-Cre* mice. (**B-M**) Mesenchymal induction of activated *Kras*^{G12D} by *Wnt1-Cre* in the *Ugdh*^{CKO}*; LSL-Kras*^{G12D} mutants failed to rescue lacrimal gland budding (D,H,L, arrows). By contrast, epithelial expression of *Hras*^{G12V} led to lacrimal gland budding in the *Ugdh*^{CKO}*; Tg-Hras*^{G12V} embryos (E,I,M, arrows). (**N**) Lacrimal gland budding rates.

induction of lacrimal gland development was observed in the *Ugdh*^{CKO}*; LSL-Kras*^{G12D} mutants (Fig. 6D,H,L, arrows). By contrast, we observed robust budding of the lacrimal gland in *Ugdh*^{CKO}*; Tg-Hras*^{G12V} embryos (Fig. 6E,I,M, arrows). These results support that the loss of epithelial FGF signaling is the ultimate cause of the lacrimal gland defects in mesenchymal knockouts of *Ugdh*.

The *N*-sulfation, but not the 2-*O*- and 6-*O*-sulfation, of mesenchymal HS was required for lacrimal gland development

Heparan sulfates are known to physically interact with FGF ligands, making this group of GAGs likely candidates for controlling Fgf10 diffusion in the periocular mesenchyme. However, we have previously shown that lacrimal gland development requires Ndst1, a major *N*-sulfation enzyme for HS, only in the conjunctival epithelium but not in the periocular mesenchyme (Pan et al., 2008). Indeed, we confirmed that *Wnt1-Cre* mediated ablation of *Ndst1* (*Wnt1-Cre; Ndst1*$^{flox/flox}$ or *Ndst1*^{CKO}) disrupted both 10E4 staining of HS and the LACE signal of Fgf10/Fgfr2b binding in the mesenchyme, but this conditional knockout of *Ndst1* did not affect lacrimal gland budding (Fig. 7A-H, arrows; *n*=5). To further investigate the role of HS in lacrimal gland development, we generated a combined deletion of both *Ndst1* and *Ndst2* (*Wnt1-Cre; Ndst1*$^{flox/flox}$*; Ndst2*$^{KO/KO}$ or *Ndst1/2*^{CKO}). Although the staining of the pan-HS marker 3G10 was unaffected, lacrimal gland budding was completely abolished in *Ndst1/2*^{CKO} mutants (Fig. 7I-L, arrows; *n*=6), demonstrating that the *N*-sulfated HS in the mesenchyme were indeed required for lacrimal gland development. We have also previously shown that lacrimal gland Fgf10 signaling requires 6-*O* and 2-*O* sulfated HS in the conjunctival epithelium (Qu et al., 2011b). Interestingly, a *Wnt1-Cre*-mediated ablation of two HS 6-*O* sulfotransferases (*Hs6st1* and *Hs6st2*) and 2-*O* sulfotransferase (*Hs2st*) did not affect HS 3G10 and 10E4 staining, but abolished Fgf10/Fgfr2b binding in the periocular mesenchyme (Fig. 7M-O, arrows). Nevertheless, lacrimal gland budding was preserved in this triple mutant (*Wnt1-Cre;Hs6st1*$^{flox/flox}$*; Hs6st2*$^{KO/KO}$*; Hs2st*$^{flox/flox}$ or *Hs6st*^{CKO}*; Hs2st*^{CKO}) (Fig. 7P, arrows; *n*=7). Consistent with this, there was no statistically significant difference in the range of Fgf10 diffusion between the control and *Hs6st*^{CKO}*; Hs2st*^{CKO} mutants (supplementary material Fig. S1). Taken together, these results support that Fgf10 signaling in lacrimal gland development requires distinctive sets of HS modifications in the epithelium and mesenchyme.

DISCUSSION

In this study, we have used lacrimal gland development as a model to study the role of GAGs in epithelium-mesenchyme interaction. We showed that mesenchymal ablation of *Ugdh* eliminated the biosynthesis of HS and CS, two major constituents of GAGs, but it did not affect the differentiation of the periocular mesenchyme. Importantly, the expression of *Fgf10* transcripts and protein was preserved in the *Ugdh* mutant mesenchyme, but the Fgf10 signaling response was lost in the lacrimal gland epithelium. Ex vivo explant experiments suggested that the loss of GAGs leads to unrestricted dispersion of Fgf10, which became too diluted in the mesenchyme to induce significant FGF signaling and budding response in the epithelium. Indeed, we showed that *Ugdh* lacrimal budding defects could be rescued by activated Ras signaling in the epithelium but not in the mesenchyme, demonstrating a non-cell-autonomous function of GAGs in the periocular mesenchyme to promote lacrimal gland development. Finally, we showed that the *Ugdh* lacrimal defect was phenocopied by the simultaneous ablation of HS modification enzymes, *Ndst1* and *Ndst2*. This shows that HS is probably the most crucial GAG regulating Fgf10 dispersion in the periocular mesenchyme.

Our study thus shows that a complete elimination of GAGs, including HS, in the ligand-producing mesenchyme abolished FGF signaling in the receptor-expressing epithelium. At first glance, this conclusion might appear contradictory to previous studies that showed gain-of-function phenotypes in *Fgf* mutants with reduced affinity to HS (Harada et al., 2009; Makarenkova et al., 2009). Here, we would like to argue that both observations were parts of the continuum of the FGF signaling response as a result of the perturbation in FGF-GAG interactions. As shown in Fig. 8, we propose that the strong affinity of wild-type FGF to extracellular

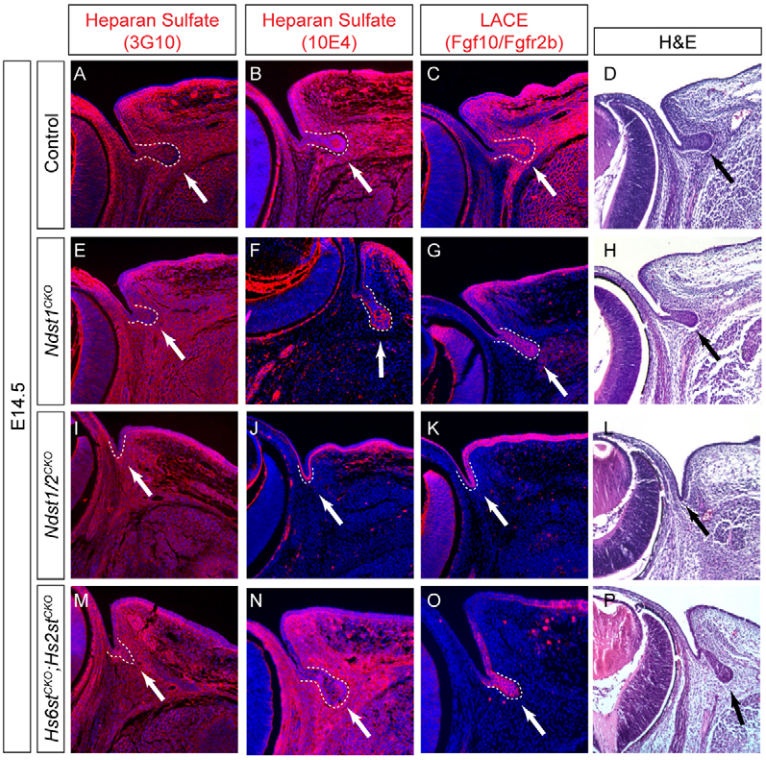

Fig. 7. Mesenchymal ablation of *Ndst1/2*, but not *Hs6st/Hs2st*, disrupted lacrimal gland budding. (**A-H**) Mesenchymal deletion of *Ndst1* (*Wnt1-Cre; Ndst1*$^{flox/flox}$ or *Ndst1*^{CKO}) disrupted both HS 10E4 staining and the Fgf10/Fgfr2b LACE signal, but lacrimal gland budding was unaffected. (**I-L**) Combined mesenchymal deletion of both *Ndst1* and *Ndst2* (*Wnt1-Cre; Ndst1*$^{flox/flox}$; *Ndst2*$^{KO/KO}$ or *Ndst1/2*^{CKO}) did not affect HS 3G10 staining but abolished lacrimal gland budding. (**M-P**) Combined deletion of *Hs6st1*, *Hs6st2* and *Hs2st* genes (*Wnt1-Cre; Hs6st1*$^{flox/flox}$; *Hs6st2*$^{KO/KO}$; *Hs2st*$^{flox/flox}$ or *Hs6st*^{CKO}; *Hs2st*^{CKO}) failed to disrupt HS 3G10 and 10E4 staining, but it did abrogate the Fgf10/Fgfr2b LACE signal. However, lacrimal gland budding was not affected.

GAGs significantly restricts the dispersion of FGFs, resulting in a steep concentration gradient away from the signal source. By contrast, *Fgf* mutants with reduced GAG affinity exhibit a shallower gradient profile, effectively expanding the range of the FGF signaling response. Elimination of all GAGs, however, leads to a free diffusion of FGFs, which are dispersed too widely to maintain a concentration high enough for lacrimal gland induction. Notably, in vivo imaging in zebrafish showed that the movement of some, but not all, Fgf8 molecules were restricted by HS in the extracellular matrix, and enzymatic degradation of HS indeed extended the range of Fgf8 signaling (Yu et al., 2009). Our study is also consistent with studies in chick and mouse, which demonstrate an essential role of HS in regulating retention versus dispersion of FGFs in embryonic development (Chen et al., 2009; Shimokawa et al., 2011). We would also like to point out that Shimokawa and colleagues recently reported that proteolytic cleavage of HS core proteins was necessary for the spread of FGFs in the extra-embryonic ectoderm (Shimokawa et al., 2011). However, it is not clear how widely applicable this mechanism of FGF transport is beyond early gastrulation, as we did not observe any visible dispersion of HS in our conditional knockouts. Although further studies are required to resolve these issues, it is clear that manipulations of FGF-HS interactions could produce both gain- and loss-of-function responses in FGF signaling.

Finally, our studies also revealed the unique sulfation requirement of mesenchymal HS in lacrimal gland development. Although the mesenchymal knockout of *Ndst1* completely abolished the 10E4 staining of HS, only the combined deletion of

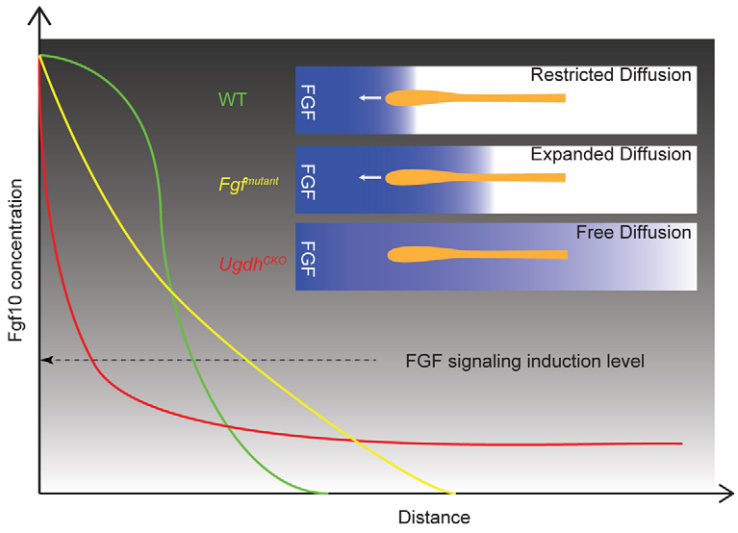

Fig. 8. Model of a biphasic regulation of FGF signaling by mesenchymal GAGs. Wild-type GAGs restrict the diffusion of FGF to a sharp concentration gradient (green line), whereas *Fgf* mutations that weaken the interaction between Fgf and GAGs produced a relatively shallow gradient (yellow line), which expanded the Fgf signaling range. By contrast, ablation of GAGs leads to a free diffusion of Fgf in the mesenchyme (red line), the concentration of which was reduced too rapidly to sustain the FGF signaling response in the epithelium. WT, wild type.

both *Ndst1* and *Ndst2* would disrupt lacrimal gland development. The 10E4 antibody is widely used to probe tissue-specific expression of HS, but our results suggest that the HS epitope recognized by this antibody is dispensable in the mesenchyme for lacrimal gland development. This is in contrast to the lacrimal gland epithelium, where we showed earlier that ablation of *Ndst1* was sufficient to abrogate lacrimal gland FGF signaling (Pan et al., 2008). The distinct sulfation requirement of HS between the epithelium and mesenchyme is also clear from analysis of HS 2-*O* and 6-*O* sulfations. Ashikari-Hada and colleagues have previously reported that Fgf10 requires 6-*O* but not 2-*O* sulfate groups for interaction with octasaccharides in vitro (Ashikari-Hada et al., 2004). However, our genetic analysis showed that lacrimal gland epithelium requires both 2-*O* and 6-*O* sulfated HS for Fgf10-induced budding (Qu et al., 2011b). In this study, we further showed that deletion of both *Hs6st* and *Hs2st* genes in the mesenchyme abolished the Fgf10/Fgfr2b LACE staining, but it did not cause any lacrimal gland budding defects. We would therefore like to propose that the function of mesenchymal HS in lacrimal gland development is regulated by its overall sulfation level but not by its specific sulfation pattern. In this view, the loss of HS 2-*O* and 6-*O* sulfation in the mesenchyme failed to disrupt lacrimal gland budding, because as we demonstrated earlier in *Hs6st; Hs2st* knockout MEF cells, the overall sulfation level of HS was maintained by the compensatory increase in *N*-sulfation (Qu et al., 2011b). By contrast, genetic deletion of both *Ndst1* and *Ndst2* has been shown to not only abolish HS *N*-sulfation, but also result in pleiotropic reduction in both HS 2-*O* and 6-*O* sulfation (Holmborn et al., 2004). Thus, for mesenchymal HS, it is the overall sulfation that is critical for lacrimal gland development.

The requirement of a sulfation level for HS in the mesenchyme is also consistent with its role in the restriction of Fgf10 diffusion during lacrimal gland development. It is likely that the electrostatic interaction between Fgf10 and the negatively charged HS dictated by its sulfation level is sufficient to confine mesenchymal Fgf10 to the vicinity of the lacrimal gland epithelium. Yet the epithelial HS are expected to participate in a trimeric complex with FGF/FGFR as a co-receptor, which might place more stringent requirements for the sulfation pattern of HS. Therefore, there is a distinctive requirement for HS fine structures in the lacrimal gland epithelium versus the mesenchyme. Differential patterns of HS modifications have also been widely observed in both normal tissues and tumors. We would like to suggest that these dynamic expressions of HS reflect their distinct functional requirement in epithelial-mesenchymal interactions, which might be important for understanding not only embryonic development but also tumorigenesis.

Acknowledgements
The authors thank Drs Wellington V. Cardoso, Jeffrey D. Esko, Valerie Dupé, Anthony Firulli, Bridget Hogan, Lena Kjellén, Richard Lang and Paul A. Overbeek for mice and reagents; Kristina Hertzler-Schaefer for critical reading of the manuscript; and members of the Zhang lab for discussions.

Funding
The work was supported by the National Institutes of Health [EY018868] and by the Ralph W. and Grace M. Showalter Research Trust Fund to X.Z. Deposited in PMC for release after 12 months.

Competing interests statement
The authors declare no competing financial interests.

Supplementary material
Supplementary material available online at
http://dev.biologists.org/lookup/suppl/doi:10.1242/dev.079236/-/DC1

References

Allen, B. L. and Rapraeger, A. C. (2003). Spatial and temporal expression of heparan sulfate in mouse development regulates FGF and FGF receptor assembly. *J. Cell Biol.* **163**, 637-648.
Ashikari-Hada, S., Habuchi, H., Kariya, Y., Itoh, N., Reddi, A. H. and Kimata, K. (2004). Characterization of growth factor-binding structures in heparin/heparan sulfate using an octasaccharide library. *J. Biol. Chem.* **279**, 12346-12354.
Bao, X., Nishimura, S., Mikami, T., Yamada, S., Itoh, N. and Sugahara, K. (2004). Chondroitin sulfate/dermatan sulfate hybrid chains from embryonic pig brain, which contain a higher proportion of L-iduronic acid than those from adult pig brain, exhibit neuritogenic and growth factor binding activities. *J. Biol. Chem.* **279**, 9765-9776.
Beer, H. D., Florence, C., Dammeier, J., McGuire, L., Werner, S. and Duan, D. R. (1997). Mouse fibroblast growth factor **10**, cDNA cloning, protein
Burgess, D., Zhang, Y., Siefker, E., Vaca, R., Kuracha, M. R., Reneker, L., Overbeek, P. A. and Govindarajan, V. (2010). Activated Ras alters lens and corneal development through induction of distinct downstream targets. *BMC Dev. Biol.* **10**, 13.
Cai, Z., Feng, G. S. and Zhang, X. (2010). Temporal requirement of the protein tyrosine phosphatase Shp2 in establishing the neuronal fate in early retinal development. *J. Neurosci.* **30**, 4110-4119.
Campbell, R. E., Mosimann, S. C., van De Rijn, I., Tanner, M. E. and Strynadka, N. C. (2000). The first structure of UDP-glucose dehydrogenase reveals the catalytic residues necessary for the two-fold oxidation. *Biochemistry* **39**, 7012-7023.
Carbe, C., Hertzler-Schaefer, K. and Zhang, X. (2012). The functional role of the Meis/Prep-binding elements in Pax6 locus during pancreas and eye development. *Dev. Biol.* **363**, 320-329.
Chen, Y., Mohammadi, M. and Flanagan, J. G. (2009). Graded levels of FGF protein span the midbrain and can instruct graded induction and repression of neural mapping labels. *Neuron* **62**, 773-780.
Danielian, P. S., Muccino, D., Rowitch, D. H., Michael, S. K. and McMahon, A. P. (1998). Modification of gene activity in mouse embryos in utero by a tamoxifen-inducible form of Cre recombinase. *Curr. Biol.* **8**, 1323-1326.
David, G., Bai, X. M., Van der Schueren, B., Cassiman, J. J. and Van den Berghe, H. (1992). Developmental changes in heparan sulfate expression: in situ detection with mAbs. *J. Cell Biol.* **119**, 961-975.
Dowd, C. J., Cooney, C. L. and Nugent, M. A. (1999). Heparan sulfate mediates bFGF transport through basement membrane by diffusion with rapid reversible binding. *J. Biol. Chem.* **274**, 5236-5244.
Entesarian, M., Matsson, H., Klar, J., Bergendal, B., Olson, L., Arakaki, R., Hayashi, Y., Ohuchi, H., Falahat, B., Bolstad, A. I. et al. (2005). Mutations in the gene encoding fibroblast growth factor 10 are associated with aplasia of lacrimal and salivary glands. *Nat. Genet.* **37**, 125-127.
Esko, J. D. and Selleck, S. B. (2002). Order out of chaos: assembly of ligand binding sites in heparan sulfate. *Annu. Rev. Biochem.* **71**, 435-471.
Forsberg, E., Pejler, G., Ringvall, M., Lunderius, C., Tomasini-Johansson, B., Kusche-Gullberg, M., Eriksson, I., Ledin, J., Hellman, L. and Kjellen, L. (1999). Abnormal mast cells in mice deficient in a heparin-synthesizing enzyme. *Nature* **400**, 773-776.
Grobe, K., Inatani, M., Pallerla, S. R., Castagnola, J., Yamaguchi, Y. and Esko, J. D. (2005). Cerebral hypoplasia and craniofacial defects in mice lacking heparan sulfate Ndst1 gene function. *Development* **132**, 3777-3786.
Hacker, U., Nybakken, K. and Perrimon, N. (2005). Heparan sulphate proteoglycans: the sweet side of development. *Nat. Rev. Mol. Cell Biol.* **6**, 530-541.
Harada, M., Murakami, H., Okawa, A., Okimoto, N., Hiraoka, S., Nakahara, T., Akasaka, R., Shiraishi, Y., Futatsugi, N., Mizutani-Koseki, Y. et al. (2009). FGF9 monomer-dimer equilibrium regulates extracellular matrix affinity and tissue diffusion. *Nat. Genet.* **41**, 289-298.
Holmborn, K., Ledin, J., Smeds, E., Eriksson, I., Kusche-Gullberg, M. and Kjellen, L. (2004). Heparan sulfate synthesized by mouse embryonic stem cells deficient in NDST1 and NDST2 is 6-O-sulfated but contains no N-sulfate groups. *J. Biol. Chem.* **279**, 42355-42358.
Hou, S., Maccarana, M., Min, T. H., Strate, I. and Pera, E. M. (2007). The secreted serine protease xHtrA1 stimulates long-range FGF signaling in the early Xenopus embryo. *Dev. Cell* **13**, 226-241.
Izvolsky, K. I., Shoykhet, D., Yang, Y., Yu, Q., Nugent, M. A. and Cardoso, W. V. (2003). Heparan sulfate-FGF10 interactions during lung morphogenesis. *Dev. Biol.* **258**, 185-200.
Izvolsky, K. I., Lu, J., Martin, G., Albrecht, K. H. and Cardoso, W. V. (2008). Systemic inactivation of Hs6st1 in mice is associated with late postnatal mortality without major defects in organogenesis. *Genesis* **46**, 8-18.
Jemth, P., Kreuger, J., Kusche-Gullberg, M., Sturiale, L., Gimenez-Gallego, G. and Lindahl, U. (2002). Biosynthetic oligosaccharide libraries for identification of protein-binding heparan sulfate motifs. Exploring the structural diversity by screening for fibroblast growth factor (FGF)1 and FGF2 binding. *J. Biol. Chem.* **277**, 30567-30573.

Kreuger, J., Jemth, P., Sanders-Lindberg, E., Eliahu, L., Ron, D., Basilico, C., Salmivirta, M. and Lindahl, U. (2005). Fibroblast growth factors share binding sites in heparan sulphate. *Biochem. J.* **389**, 145-150.

Kreuger, J., Spillmann, D., Li, J. P. and Lindahl, U. (2006). Interactions between heparan sulfate and proteins: the concept of specificity. *J. Cell Biol.* **174**, 323-327.

Ledin, J., Staatz, W., Li, J. P., Gotte, M., Selleck, S., Kjellen, L. and Spillmann, D. (2004). Heparan sulfate structure in mice with genetically modified heparan sulfate production. *J. Biol. Chem.* **279**, 42732-42741.

Liu, P., Jenkins, N. A. and Copeland, N. G. (2003). A highly efficient recombineering-based method for generating conditional knockout mutations. *Genome Res.* **13**, 476-484.

Maccarana, M., Sakura, Y., Tawada, A., Yoshida, K. and Lindahl, U. (1996). Domain structure of heparan sulfates from bovine organs. *J. Biol. Chem.* **271**, 17804-17810.

Makarenkova, H. P., Ito, M., Govindarajan, V., Faber, S. C., Sun, L., McMahon, G., Overbeek, P. A. and Lang, R. A. (2000). FGF10 is an inducer and Pax6 a competence factor for lacrimal gland development. *Development* **127**, 2563-2572.

Makarenkova, H. P., Hoffman, M. P., Beenken, A., Eliseenkova, A. V., Meech, R., Tsau, C., Patel, V. N., Lang, R. A. and Mohammadi, M. (2009). Differential interactions of FGFs with heparan sulfate control gradient formation and branching morphogenesis. *Sci. Signal.* **2**, ra55.

Pan, Y., Woodbury, A., Esko, J. D., Grobe, K. and Zhang, X. (2006). Heparan sulfate biosynthetic gene Ndst1 is required for FGF signaling in early lens development. *Development* **133**, 4933-4944.

Pan, Y., Carbe, C., Powers, A., Zhang, E. E., Esko, J. D., Grobe, K., Feng, G. S. and Zhang, X. (2008). Bud specific N-sulfation of heparan sulfate regulates Shp2-dependent FGF signaling during lacrimal gland induction. *Development* **135**, 301-310.

Pan, Y., Carbe, C., Powers, A., Feng, G. S. and Zhang, X. (2010). Sprouty2-modulated Kras signaling rescues Shp2 deficiency during lens and lacrimal gland development. *Development* **137**, 1085-1093.

Patel, V. N., Knox, S. M., Likar, K. M., Lathrop, C. A., Hossain, R., Eftekhari, S., Whitelock, J. M., Elkin, M., Vlodavsky, I. and Hoffman, M. P. (2007). Heparanase cleavage of perlecan heparan sulfate modulates FGF10 activity during ex vivo submandibular gland branching morphogenesis. *Development* **134**, 4177-4186.

Qu, X., Hertzler, K., Pan, Y., Grobe, K., Robinson, M. L. and Zhang, X. (2011a). Genetic epistasis between heparan sulfate and FGF-Ras signaling controls lens development. *Dev. Biol.* **355**, 12-20.

Qu, X., Carbe, C., Tao, C., Powers, A., Lawrence, R., van Kuppevelt, T. H., Cardoso, W. V., Grobe, K., Esko, J. D. and Zhang, X. (2011b). Lacrimal gland development and Fgf10-Fgfr2b signaling are controlled by 2-O- and 6-O-sulfated heparan sulfate. *J. Biol. Chem.* **286**, 14435-14444.

Shimokawa, K., Kimura-Yoshida, C., Nagai, N., Mukai, K., Matsubara, K., Watanabe, H., Matsuda, Y., Mochida, K. and Matsuo, I. (2011). Cell surface heparan sulfate chains regulate local reception of FGF signaling in the mouse embryo. *Dev. Cell* **21**, 257-272.

Sommer, B. J., Barycki, J. J. and Simpson, M. A. (2004). Characterization of human UDP-glucose dehydrogenase. CYS-276 is required for the second of two successive oxidations. *J. Biol. Chem.* **279**, 23590-23596.

Stanford, K. I., Wang, L., Castagnola, J., Song, D., Bishop, J. R., Brown, J. R., Lawrence, R., Bai, X., Habuchi, H., Tanaka, M. et al. (2010). Heparan sulfate 2-O-sulfotransferase is required for triglyceride-rich lipoprotein clearance. *J. Biol. Chem.* **285**, 286-294.

Taylor, K. R., Rudisill, J. A. and Gallo, R. L. (2005). Structural and sequence motifs in dermatan sulfate for promoting fibroblast growth factor-2 (FGF-2) and FGF-7 activity. *J. Biol. Chem.* **280**, 5300-5306.

Tuveson, D. A., Shaw, A. T., Willis, N. A., Silver, D. P., Jackson, E. L., Chang, S., Mercer, K. L., Grochow, R., Hock, H., Crowley, D. et al. (2004). Endogenous oncogenic K-ras(G12D) stimulates proliferation and widespread neoplastic and developmental defects. *Cancer Cell* **5**, 375-387.

van den Born, J., Salmivirta, K., Henttinen, T., Ostman, N., Ishimaru, T., Miyaura, S., Yoshida, K. and Salmivirta, M. (2005). Novel heparan sulfate structures revealed by monoclonal antibodies. *J. Biol. Chem.* **280**, 20516-20523.

van Kuppevelt, T. H., Dennissen, M. A., van Venrooij, W. J., Hoet, R. M. and Veerkamp, J. H. (1998). Generation and application of type-specific anti-heparan sulfate antibodies using phage display technology. Further evidence for heparan sulfate heterogeneity in the kidney. *J. Biol. Chem.* **273**, 12960-12966.

Yan, D. and Lin, X. (2007). Drosophila glypican Dally-like acts in FGF-receiving cells to modulate FGF signaling during tracheal morphogenesis. *Dev. Biol.* **312**, 203-216.

Yu, S. R., Burkhardt, M., Nowak, M., Ries, J., Petrasek, Z., Scholpp, S., Schwille, P. and Brand, M. (2009). Fgf8 morphogen gradient forms by a source-sink mechanism with freely diffusing molecules. *Nature* **461**, 533-536.

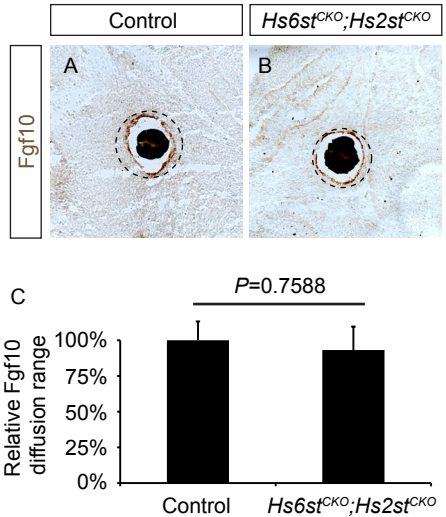
Control
Hs6st^CKO;Hs2st^CKO
Fgf10
A
B
C
P=0.7588
Relative Fgf10 diffusion range
100%
75%
50%
25%
0%
Control
Hs6st^CKO;Hs2st^CKO